International Journal of Advance Research in Science and Engineering
Vol. No.4, Special Issue No. (01), December 2015
www.ijarse.com
IJARSE
ISSN 2319 - 8354

FERROELECTRIC RELAXOR BEHAVIOUR AND DIELECTRIC RELAXATION IN $Sr_{0.25}Ba_{0.75}Nb_2O_6$ A LEAD FREE RELAXOR MATERIAL

K.N. Singh[1], Santosh Agrawal[2], P.K. Bajpai[3]

[1,2]Department of Physics Dr. C.V. Raman University Kota, Bilaspur (C.G.) (India)

[3]Advance Research Laboratory, Department of Pure & Applied Physics

Guru Ghasidas University, Bilaspur (India)

ABSTRACT

Controlling the cooling rate during calcination and optimizing sintering temperature have prepared single phase pure **$Sr_{0.25}Ba_{0.75}Nb_2O_6$** ceramics are synthesized by simple solid state reaction route. Material calcined at 1250^0C and sintered at 1300^0C stabilized in pure phase with tetragonal structure having density >95%. Lattice parameters for SBN25 (a= 12.467(4) A^0, c=3.956(5) A^0). The composition shows a relaxor-type behaviour with diffuse phase transition. Modified Curie-Weiss law is used to fit the dielectric data. The dielectric relaxation obeys the Vogel–Fulcher relationship with the freezing temperature 277.3K for SBN25. Significant dielectric dispersion is observed in low frequency regime in both components of dielectric permittivity and a small dielectric relaxation peak is observed in the temperature range (323-473K). This is associated with defect related hopping process.

Keywords: Dielectric Relaxation, Relaxors, Vogel-Fulcher Relation

I. INTRODUCTION

Strontium barium niobate, $(Sr_xBa_{1-x})Nb_2O_6$ (SBN) have remarkable ferroelectric properties [1], pyroelectric, linear electro-optic coefficients [2] and strong photorefractive effects [3] and have widely been applied in technological applications like storage media for holograms [4], pyroelectric [5] and piezoelectric [6] applications, and electro-optic data storage [7]. SBN crystallizes in a tetragonal tungsten bronze structure, space group *P4bm* [8]. Ferroelectric SBN materials are stable since they contain no volatile element such as Pb [9, 10] in perovskite ferroelectrics. Although SBN single crystals are preferable for these applications, high cost and difficult fabrication limits its practical use [11]. SBN ceramics have advantage of low cost, easy synthesis and would be promising alternate for many of the applications. For optical and ferroelectric application, high density and improved dielectric properties is greatly desired [12-14]. The use of solution based chemical synthesis methods ensures atomic level mixing of the reactants and hence can circumvent the high calcination temperature requirements associated with the conventional solid-state methods. Unfortunately, the preparation of dense SBN ceramics through chemical synthesis methods gets complicated [15] by the moisture sensitivity and easy hydrolysis of the niobium sources [16-18]. Therefore, controlling the processing and parameters in simple solid state route to attain high density single phase seems to be the possible way.

We, therefore, synthesized solid solutions $Sr_{0.25}Ba_{0.75}Nb_2O_6$ abbreviated as SBN25 in simple solid state reaction route and studied the ferroelectric relaxor behaviour and dielectric relaxation in these important ceramics compositions. To the best of our knowledge, no such detailed report exists in literature.

II. EXPERIMENTAL PROCEDURE

$Sr_{0.25}Ba_{0.75}Nb_2O_6$ is synthesized by taking stoichiometric amounts of high purity powder of $SrCO_3$ (Loba-99.9%), $BaCO_3$ (Loba-99.9%) and Nb_2O_5 (Loba-99.5%) using solid-state reaction route. The stoichiometric amounts of constituent's powders were wet mixed in acetone for 6 hours. The mixed powders were calcined at an optimum calcination temperature (1250^{o}C) for 5 hours at the rate of 2^{0}C/m. Calcined powders were structurally analyzed by X-ray diffraction technique using X-ray diffractometer (Rigaku, Miniflex). Fine calcined powders were pressed into cylindrical pellets of 10 mm diameter and 1-2 mm thickness under an iso-static pressure of 100 MPa. Polyvinyl alcohol (PVA) was used as a binder. The pellets were sintered at 1300^{o}C temperatures, for 4 hours and cooled down to room temperature using controlled cooling rate 2^{0}C/minute. The phase formation has been identified using X-ray diffraction analysis again**.** To measure the dielectric properties, sintered pallets were electroded with silver paste and heated at 500^{0}C for 1 hour and cooled down up to room temperature before measurements were performed. The dielectric data were taken in the temperature range (30–350^{0}C) and at the heating rate of 2^{0}C min^{-1}. The dielectric data were recorded using HIOKI 3532 LCR Hi TESTER impedance analyzer. P-E data were recorded using P-E loop tracer (Marine India Pvt. Limited).

III. RESULTS AND DISCUSSION

3.1 X-ray Diffraction Study

Figure 1 shows the X-ray diffraction profile of SBN25. The compositions have been confirmed as single phases with tetragonal structure by indexing observed XRD peaks using an XRD interpretation and indexing program POWD [19]. The unit cell parameters were refined using the criteria that the sum of difference between observed (d_{obs}) and calculated (d_{cal}) interplaner spacing $\Sigma\Delta d = \Sigma (d_{obs}-d_{cal})$ is minimum. SBN25 stabilize in tetragonal structure with lattice parameters a= 12.467(4) A^0, c=3.956(5) A^0, These values are very close to earlier report (JCPDF-39-0265). The particle size was determined using Scherer formula and is ≈ 390A^0 (SBN25).

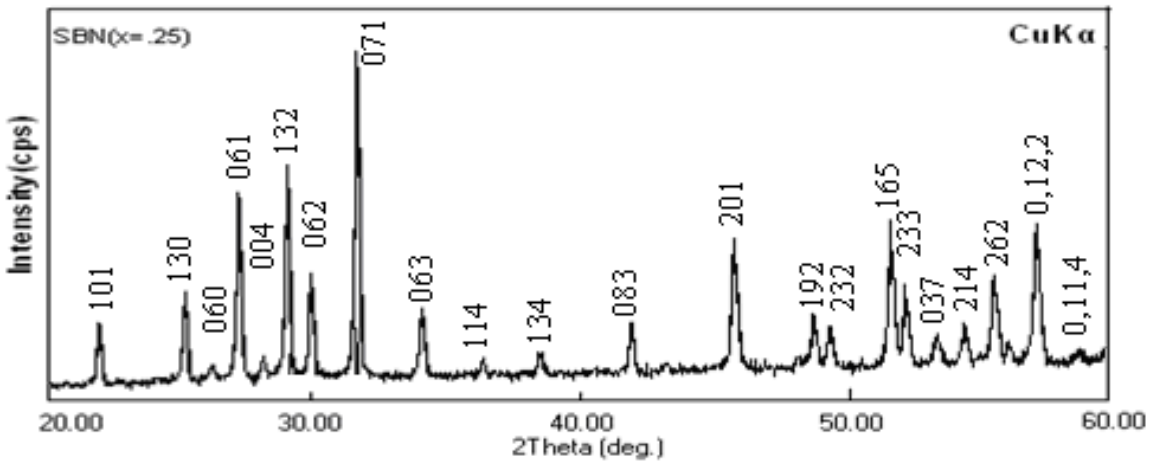

Figure: 1. X-RD pattern of $Sr_{0.25}Ba_{0.75}Nb_2O_6$.

SBN25 has a tungsten bronze type of structure [20-22], with unit cell formula of $(A_1)_2\,(A_2)_4\,C_4B_{10}O_{30}$, in which A_1, A_2, C and B cations are in the 15-, 12-, 9-,6- coordinated sites, respectively. The Ba^{2+} ion predominantly occupies the 15- fold-coordinated sites as the radius of Ba^{2+} ion ($1.74A^0$) is substantially larger than that of the Sr^{2+} ion ($1.44A^0$). Therefore, the Sr^{2+} ion occupies either the A_2 or a combination of A_1- and A_2 - sites. As the Sr/Ba ratio is increased more Sr^{2+} occupies A_2- sites. Considering the ionic radius of Ba^{2+} larger than Sr^{2+}. The formation of pure TTB phase in SBN25 at relatively lower sintering temperature 1300^0C and higher densification (>95% density) is achieved in the present studies in comparison to 1350^0C (92% density) as reported by Qu.et.al [23] or 1400^0C as reported by Ho. et.al. [24] is significant as it may reduce the problem of abnormal grain growth, occurring due to high sintering temperatures. It is to be noted that electrical and optical properties are deteriorated due to abnormal grain growth.

3.2 Dielectric Study

For SBN25 solid solution temperature dependence of dielectric constants (ε') shows a broad maximum (Fig 2) which is shifted to higher temperature for raising frequencies, whereas its maximum value (ε'_m) decreases. A frequency dispersion takes place at $T < T_m$.

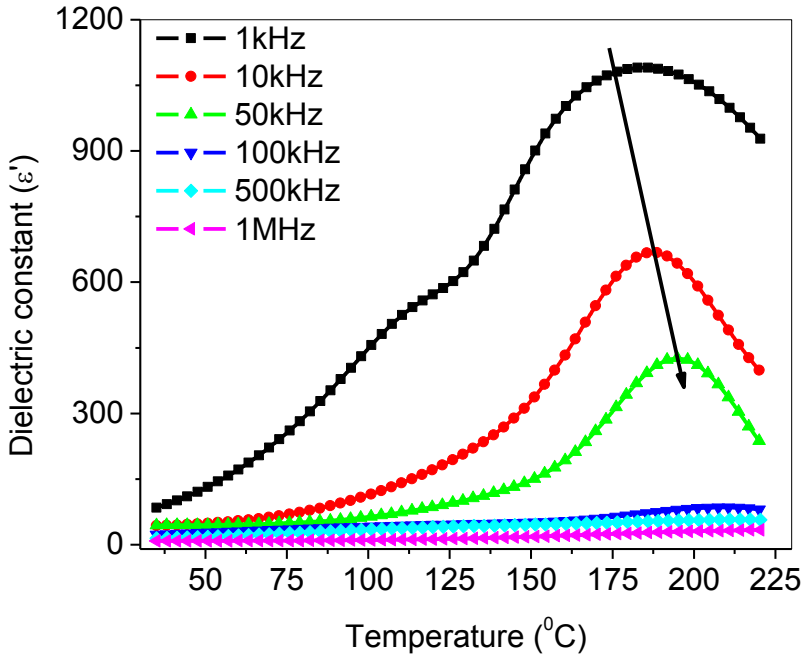

Figure: 2 Temperature dependence of dielectric constant of SBN25.

The temperature and frequency dependence of dielectric loss (tanδ) plotted in Figures 3. A shift of the temperature T'_m of tanδ to higher values for raising frequencies is observed. Further T_m of (ε'_m) and T'_m of (tanδ) do not coincide at a given frequency. Transition temperature decreases with increase in Sr content in SBN. The maximum relative permittivity (ε'_m) as well as its corresponding temperature (T_m) is given in table 1. Hence, these results suggest that the dielectric polarization has relaxation-type behaviour and composition to be of relaxor type. However, significant frequency dispersion is seen in ε' for temperatures $T > T_m$ also, unlike classical relaxor materials. This may be associated with increased distortion in SBN25 ceramics as is well known that with different Sr/Ba ratio.

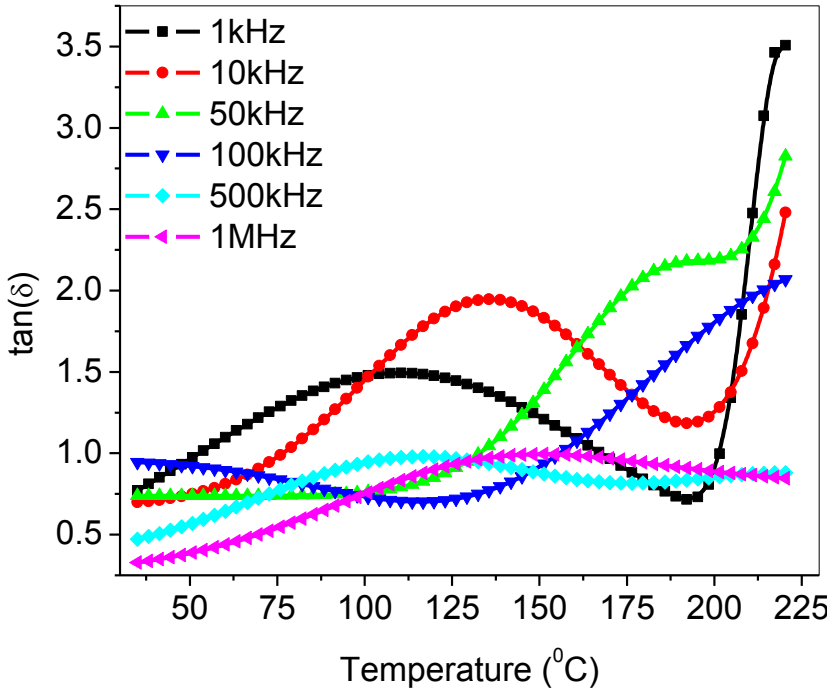

Figure: 3 shows temperature dependence of tangent loss of SBN25.

Table 1 Maximum temperature (T_m) and peak dielectric constant values (ε'_m) at representative frequencies in different compositions of SBN25.

Frequency (kHz)	SBN25	
	T_m(K)	ε'_m
1	448	1100
5	463	687
10	468	432
50	483	89
100	493	58

To analyze the observed diffuse phase transition characteristics further, frequency dispersion) (ΔT_m) and the diffusivity (γ) are used to reflect the relaxor behavior of the studied ceramics. It is well known that the dielectric constant for normal ferroelectrics above the Curie temperature follows the Curie–Weiss law [25] described by

$$\frac{1}{\varepsilon'} = \frac{(T-\Theta)}{C} \quad (T > T_c) \qquad (1)$$

where Θ is the Curie temperature and C is the Curie constant. The Curie–Weiss plot between (1/ε' vs. temperature) gives a straight line with a slope of (1/C) and the X-axis intercept at Θ.

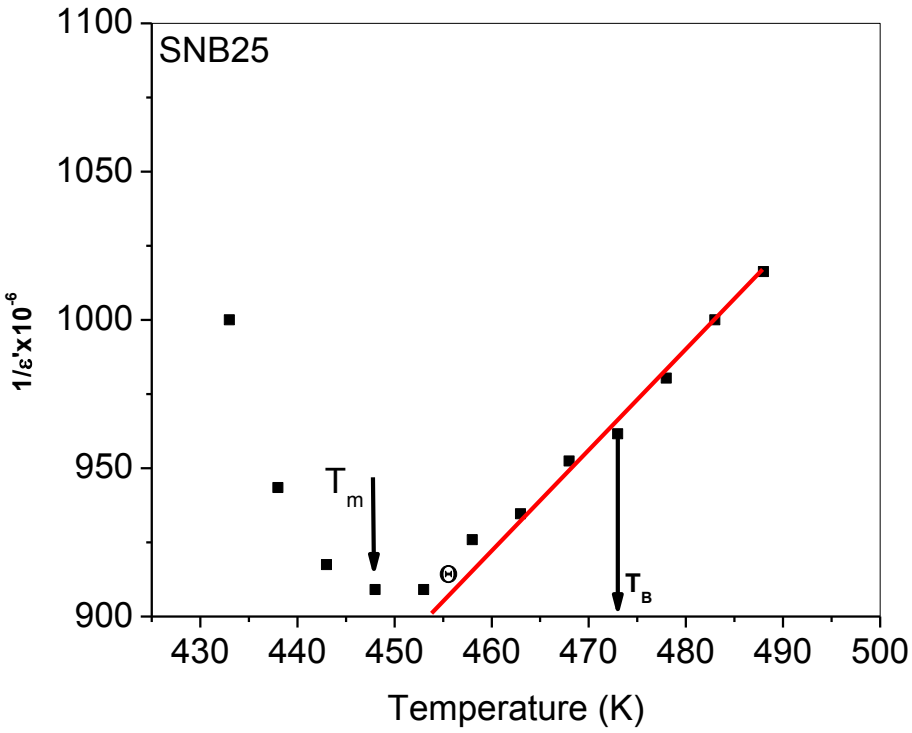

Figure: 3 Temperature dependence of the reciprocal dielectric constant (1/ε ′) for SBN25.

Fig. 3 show the Curie–Weiss plot for SBN25 at 1 kHz. The degree of deviation from the Curie–Weiss behavior could be given by ΔT_m, where

$$\Delta T_m = T_B - T_m \qquad (2)$$

where T_B represents the temperature from which ε' starts to deviate from the Curie–Weiss law, and T_m denotes the temperature of dielectric permittivity maximum (ε'_m) . The difference between two temperatures, (T_B- T_m), could be used to characterize diffuseness of phase transition [26]. At 1 kHz, ΔT_m = 25 K for SBN25. The Curie temperature Θ, the Burn temperature, T_B and the temperature difference (T_B - T_m) are summarized in table 2 for both compositions.

Table 2 Characteristic parameters determined and calculated from ε′(T) measurements.

Sample	Frequency(KHz)	T_m(K)	Θ(K)	T_B(K)	$\Delta T_m=T_B-T_m$
SBN25	1	448	456	473	25

Another parameter $\Delta T_{m\,(relax)}$ is used to characterize the degree of relaxation behavior in the frequency range of 1 kHz to 100 kHz, described [27] as

$$\Delta T_{m\,(relax)} = T_{m\,(100\ kHz)} - T_{m\,(1\ kHz)} \qquad (3)$$

$\Delta T_{m\,(relax)}$, obtained from the dielectric measurements (table 1) is approximately 45K for SBN25.

The dielectric behavior of a relaxor ferroelectric could be described by a modified Curie–Weiss law given by [28],

$$\frac{1}{\varepsilon'} - \frac{1}{\varepsilon'_m} = \frac{(T - T_m)^{\gamma}}{C'} \qquad (4)$$

where γ and C' are measured to be constants, the value of γ lies between 1 and 2 . The parameter γ gives information on the phase transition character; γ =1 represents classical ferroelectric phase transition where normal Curie-Weiss law is followed and γ =2 gives the quadratic dependence which describes complete diffuse phase transition. Figure 4 shows the plot of log $(1/\varepsilon - 1/\varepsilon_m)$ vs. log $(T-T_m)$ at 1kHz for SBN25. A linear relationship is obvious from the plot. The value of γ estimated from the slope of the graphs is 1.25, for SBN25, indicating that the materials have diffuse phase transition characteristics.

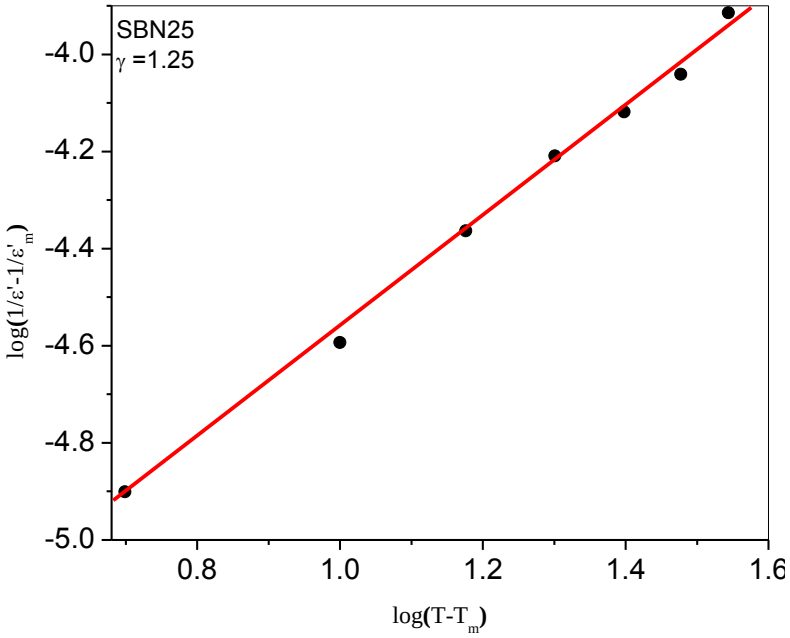

Figure 4 log $(1/\varepsilon - 1/\varepsilon_m)$ as function of log$(T-T_m)$ for SBN25 at 1 kHz.

The observed broadness or diffuseness occurs mainly because of the compositional fluctuations and/ or due to structural disorder in the lattice. This may be correlated with the prevailing disorder at A-site due to the two cations (Ba^{2+} and Sr^{2+}) competing at this site. Thus the dielectric polarization may be similar to that observed in dipolar glasses. In analogy with spin glasses the dynamic susceptibility behavior in disordered ferroelectrics is supposed to be associated with a broad spectrum of relaxation time. Therefore, the Debye model, which is based on the single relaxation time, fails when employed for a system with distributed relaxation time.

Fig.5 shows the curve of log (ω) vs. $1/T_m$ for SBN25. A nonlinear behavior is observed indicating that the data do not obey the simple Debye equation. In order to analyze relaxor characteristics of SBN ceramics, the experimental curve (Fig. 6) was fitted using Vogel–Fulcher relation [29, 30].

$$\omega = \omega_o \exp\left[\frac{-E_a}{k_B(T_m - T_f)}\right] \qquad (5)$$

The T_f is considered as the temperature, where the dynamic reorientation of distorted $[NbO_6]$ clusters leads to polarization in the lattice.

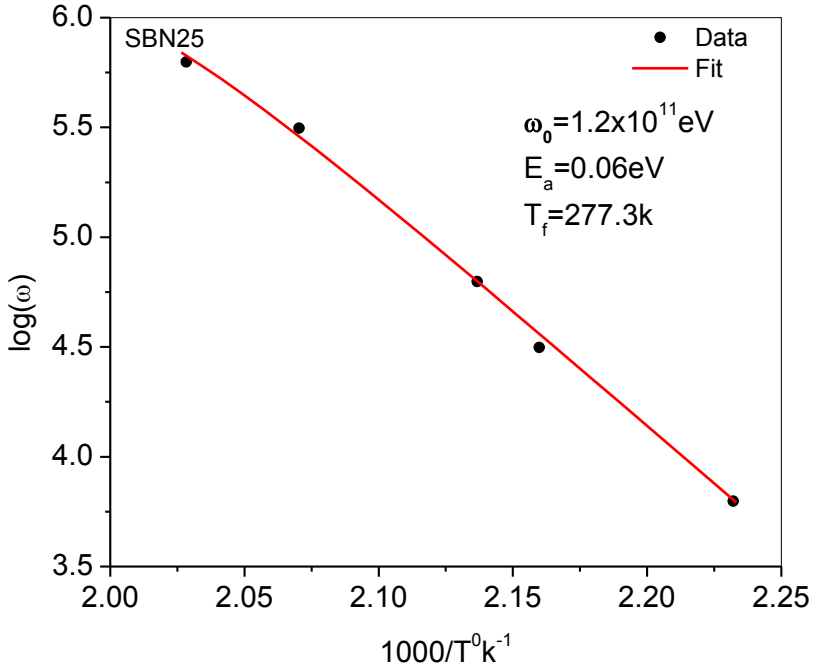

Figure: 5 log(ω) versus l/T_m plot for SBN25. The solid line represents the fitting to Vogel–Fulcher relationship.

Fig. exhibits the Vogel–Fulcher plot for the SBN compositions.

3.3 Ferroelectric Properties

Fig.6 shows polarization-electric field (P-E) hysteresis loops for SBN25 at 423K. The hysteresis loops exhibit ferroelectric-like behavior [31, 32]. The value of P_s and E_c gradually decreases with increasing Sr content.

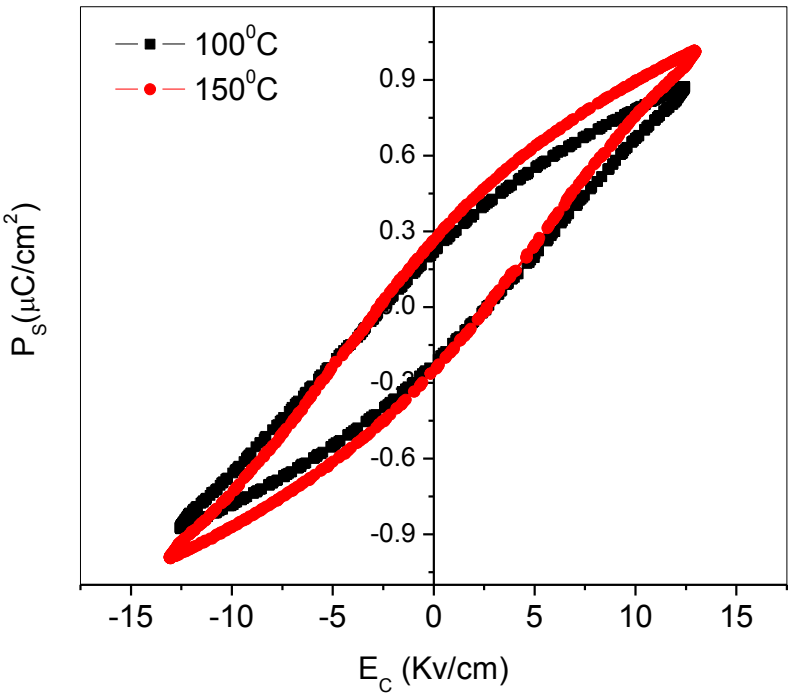

Figure 6 P–E hysteresis loops of SBN25, measured at 423K.

The observed value of spontaneous polarization (P_s) is 1.35 μC/cm^2, coercive field E_c = 13 kV/cm for SBN25 at 423K. The values of Ps are smaller than those reported earlier [33, 34].

IV. CONCLUSIONS

SBN ceramic compositions calcined at 1250^{0}C and sintered at 1300^{0}C stabilized in phase pure tetragonal structure with lattice parameters (a= 12.4674 A^0, c=3.9565 A^0), for SBN25. The phase pure ceramics are obtained at relatively low sintering temperature and with higher density (>95%) that of theoretical value. Modified Curie law is used to fit the experimental dta indicating that the compositions have diffuse phase transition characteristics with γ=1.25 SBN25. Values of the parameters T_m = 448K, T_B = 473 K and ΔT_m (=T_B - T_m) 25 for SBN25 obtained as a characteristic diffuseness of phase transition are smaller to those obtained for classical relaxors. Vogel–Fulcher relationship is found to be valid and are used to obtain characteristic parameters of diffuse phase transitions; relaxation frequency, activation energy, E_a and freezing temperature T_f .Cole-Cole plots of dielectric constant indicate polydispersive nature of the dielectric relaxation. SBN25 exhibits ferroelectric hysteresis loops with coercive fields close to those reported earlier. However, the observed spontaneous polarization is smaller than those reported as is attributed to lower sintering temperature used in the study.

REFERENCES

[1] A.M. Glass, Appl. Phys. Lett. **13,** (1968) 147.
[2] S. Sakamoto and T. Yazzki, Appl. Phys. Lett. **22,** (1973) 429.
[3] W.H. Liu, Y.S. Qiu, H.J. Zhang, J.H. Dai, P.Y. Yang and L.Y. Xu, Opt. Commun. **64,** (1987) 81.
[4] T. Kume, K. Nonaka, M. Yamamoto, Jpn. J. Appl. Phys. **35,** (1996) 448.
[5] S.T. Liu, R.B. Maciolek, J. Electron. Mater. **4,** (1975) 91.
[6] T.-T. Fang, E. Chen, W.J. Lee, J. Eur. Ceram. Soc. **20,** (2000) 527.
[7] Y.S. Yang, M.K. Rhy, H.J. Joo, S.H. Lee, S.J. Lee K.Y. Kang, M.S. Jang, Appl. Phys. Lett. **76,** (2000) 3472.
[8] P.B. Jamieson, S.C. Abrahams, J.L. Bernstein, J. Chem. Phys. **48,** (1968) 5048.
[9] H.F. Cheng, Jpn. J. Appl. Phys. **32,** (1993) 5656.
[10] H.F. Cheng, Appl. Surf. Sci. **92,** (1996) 378.
[11] Jyh-Tzong Shiue, Tsang-Tse Fang, Journal of the European Ceramic Society **22** (2002) 1705.
[12] K. Nagata, Y. Yamamoto, H. Igarashi and K. Okazaki, Ferroelectrics **38** (1981) 853.
[13] S.I. Lee and W.K. Choo, Ferroelectrics **87** (1988) 209.
[14] N.S. Vandamme, A.E. Sutherland, L. Jones, K. Bridger and S.R. Winzer, J. Am. Ceram. Soc. **74** (8) (1991) 1785.
[15] R. N. Das and P. Pramanik *Mater. Lett.* **46**, (2000) 7
[16] J. H. Choi, J. S. Woo, S. G. Hong and D. J. Kim *Mater. Res. Bull.* **25, (**1990) 283
[17] M. M. A. Sekar and A. Halliyal *J. Am. Ceram. Soc.* **81, (**1998) 380
[18] Y. Narender and G. L. Messing *J. Am. Ceram. Soc.* **80, (**1997) 915

[19] E. Wu, "POWD", an Interactive Powder Diffraction Data Interpretation and Indexing Programme, *Ver. 2.1*, Schoolof Physical Sciences, Flinders University of South Australia, Bedford Park, S.A.,5042,Australia.

[20] M.H. Francombe, Acta Crystallogr **13** (1960) 131.

[21] B. Jaffe, W.R. Cook jr, H.Jaffe, Piezoelectric Ceramic Academic Press New Yark 1971 pp. 213.

[22] A.M. Glass J. Appl.Phys. **40** (1969) 4699.

[23] M.M.T. Ho, C.L. Mak, K.H. Wong, Ferroelectrics **231** (1999) 255

[24] Yong-Quan Qu, Ai-Dong Li, Qi-Yue Shao, Yue-Feng Tang, Di Wu, C.L Mak, K.H. Wong, Nai-Ben Ming, Material Research Bulletin **37** (2002) 503

[25] L. Zhou, P.M. Vilarinho, J.L. Baptista, J. Appl. Phys. **85** (1999) 2312.

[26] L. Zhou, P.M. Vilarinho, J.L. Baptista, J. Electroceram. **5** (2000) 191.

[27] C. Ang, Z. Jing, and Z. Yu, J. Phys. Cond. Matter, **14** (2002) 8901.

[28] G. Fulcher, J. Am. Ceram. Soc. **8** (1925) 339

[29] Y. Guo, K. Kakimoto and H. Ohsato *J. Phys. Chem. Solids* **65 (**2004)1831

[30] S. K. Rout, T. Badapanda, E. Sinha, S. Panigrahi, P. K. Barhai and T. P. Sinha *Appl. Phys.* A **91 (**2008)101

[31] W. Ren, S. Trolier-McKinstry, C.A. Randall, T.R. Shrout, J. Appl. Phys. **89** (2001) 767.

[32] Z. Kighelman, D. Damjanovic, A. Seifert, L. Sagalowicz, N. Setter, Appl. Phys. Lett. **73** (1998) 2281.

[33] A.V. Murugan, A.B. Gaikwad, V. Samuel and V. Ravi, Bull. Mater. Sci., **29** (2006) 221.

[34] P.K. Patro, A.R. Kulkarni, S.M. Gupta and C.S. Harendranath, Defence Science Journal, **57** (2207) 79